

# Hydrodynamical simulations of galaxy clusters: exploring the thermodynamics of the hot intra-cluster medium

Susana Planelles<sup>1,2</sup>

<sup>1</sup> Astronomy Unit, Department of Physics, University of Trieste, via Tiepolo 11, I-34131 Trieste, Italy

<sup>2</sup> INAF, Osservatorio Astronomico di Trieste, via Tiepolo 11, I-34131 Trieste, Italy

## Abstract

Modern cosmological simulations represent a powerful means to analyse and interpret the formation and evolution of cosmic structures. The first attempts to perform such simulations, dated back to 1960-1970, consisted in N-body collisionless computations with few point masses. Since then, cosmological simulations have experienced a great progress and have increased significantly in scale and complexity. A relevant effort has been done to properly model the hydrodynamical mechanisms shaping the observational properties of galaxies and galaxy clusters. Despite the significant improvements of the last years, results from current simulations still show important deviations from observations, especially within the core regions of galaxy clusters and within the framework of galaxy formation. In this contribution, I will briefly review the current numerical methods employed in large-scale cosmological simulations. A special emphasis will be put on the effects that the inclusion of different baryonic processes, such as radiative cooling, star formation or AGN feedback, has on the physical properties of the hot intra-cluster medium of massive galaxy clusters. In addition, some of the technical and computational challenges that numerical cosmology has to overcome in the near future will be outlined.

## 1 Introduction

The spatially flat  $\Lambda$ -Cold Dark Matter model [5] represents nowadays the accepted paradigm of structure formation. Within this paradigm, the first structures in the Universe were formed by the gravitational collapse of primordial matter density fluctuations induced by inflation. Later on, the formation of cosmic structures proceeds in a hierarchical way, with the smaller objects forming larger systems via merger events and matter accretion. As a

result, a complicated network of cosmic structures interconnected along walls and filaments over a wide range of mass and spatial scales is generated. Nowadays, different observational probes have set strong constraints on the parameters describing the underlying cosmological model (e.g. [21]).

Clusters of galaxies, residing at the top of the cosmic hierarchy, are the youngest and most massive objects formed (see [17] and [26] for recent reviews). As a consequence, they represent a main part of the large scale structure of the Universe, marking the limit between cosmological and galactic scales. Galaxy clusters, with typical masses of  $10^{13}$  up to  $10^{15} M_{\odot}$ , occupy a region in the sky of typically a few megaparsecs. Most of the cluster mass is in the form of dark matter (DM;  $\sim 80\%$ ), followed by a hot baryonic component ( $\sim 15\%$ ) and cold baryons in stars and galaxies ( $\sim 5\%$ ). The hot gaseous component, with typical temperatures of  $\sim 10^7 - 10^8$  K, is enclosed within a hot and diffused plasma, called intra-cluster medium (ICM), which intensively emits in the X-ray band. The ICM, with low electron number densities ( $n_e \sim 10^{-4} - 10^{-2} \text{ cm}^{-3}$ ), contains mainly hydrogen and helium but also an average content of heavier elements at a level of about  $\sim 1/3$  of the solar abundance.

Given their composition, galaxy clusters can be observed in different wave bands. In general, observations report that the ICM is quite different from cluster to cluster. However, clusters of a given mass and at a given redshift also show some regularities. As an example, an important effort has been put on the analysis of the mean radial profiles of temperature, entropy and pressure based on observations of large samples of galaxy clusters and groups. From the analysis of these mean profiles three different regions can be distinguished within clusters: inner core regions ( $r \leq 0.2R_{500}$ ), where the average profiles show a large scatter depending on the presence and relevance of cool, dense cores; intermediate cluster regions, where the scatter is reduced and clusters behave nearly in a self-similar way; and cluster outskirts ( $r > R_{500}$ ), where the scatter increases with radius and clusters are dynamically younger, suffering from a significant merging activity and departures from equilibrium.

The existence of these radial zones allows us to understand the effects of different physical processes on the ICM thermodynamics. At intermediate cluster regions, a simple self-similar model [16], based on the hydrostatic equilibrium condition and on gravitational physics, can explain most of cluster properties. Indeed, at these scales, self-similar scaling relations between different cluster properties describe quite well observations. However, observed deviations from self-similarity in inner core regions suggest the effect of additional non-gravitational processes which play a major role in this internal domain. On the other hand, although cluster outskirts are supposed to be nearly self-similar, a number of processes can deviate them from equilibrium, producing important departures from self-similarity. These outer regions, however, still need to be observationally constrained in a precise way.

This general picture suggests that, while the ICM thermodynamics is mainly driven by gravity in outer cluster regions, non-gravitational processes acting on the baryonic component, such as star formation, radiative cooling or AGN feedback, are crucial in more internal regions. Given the complexity of the underlying scenario, hydrodynamical/N-body cosmological simulations seem to be crucial to disentangle the complex interplay between gravitational and non-gravitational physical processes responsible of the observational features of galaxy clusters.

## 2 Simulating the real Universe

In the last forty years cosmological simulations have experienced a significant improvement. The numerical progress together with the advance in computers and computational resources have converted simulations into an essential tool to improve our understanding of the Universe.

The first cosmological simulations, performed in the 1960s-1970s (e.g., [1, 19]), consisted in N-body calculations with few DM particles. Since then, N-body algorithms to model the evolution of the collisionless dark matter component have experienced a great improvement. The main objective of cosmological simulations is, however, to reproduce the observable Universe as accurately as possible. Therefore, besides DM, the evolution of the baryonic component of the Universe also needs to be properly modelled. As a consequence, any simulation trying to model the real Universe needs to include, at least, an N-body treatment for the evolution of DM coupled to a hydrodynamical approach for the evolution of baryons. The physics and dynamics of the gaseous component is however much more difficult to model than the formation of dark matter structures. The first cosmological simulations accounting for a coupled evolution of dark matter and baryons were performed in the 1980s [11, 15].

In general, cosmological simulations reduce the evolution of the Universe to an initial value problem suitable for computation. Thanks to a number of different observational probes, initial conditions for cosmological simulations can now be determined with a low degree of ambiguity. Therefore, the main challenge of simulations is to properly resolve the coupled evolution of both dark and baryonic components.

Figure 1 shows how the distributions of DM, gas and stellar density evolve as a function of redshift, as predicted by a cosmological hydrodynamical simulation performed with the **MASCLET** code [30]. This simulation assumes a spatially flat  $\Lambda$ CDM model and includes cooling, heating processes for a primordial gas, and star formation (for further details about this simulation see [22] and [23]). The evolution of the DM, gas and stellar components clearly shows the hierarchical manner in which the formation of cosmic structures proceeds: a smooth density medium at high redshift evolves into a much more filamentary and complex field at later times. At  $z = 0$ , a massive galaxy cluster has formed at the intersection of quite large filamentary structures.

### 2.1 Numerical techniques

Owing to their different nature, dark matter and baryonic components need to be evolved using different numerical techniques (see [10, 7] for recent reviews). The evolution of these components relates to each other via the global gravity field.

- Dark matter dynamics. The cold dark matter component is usually approximated by a collisionless, non-relativistic fluid of particles. The phase space is sampled by a system of N tracer particles whose equations of motion are then integrated under the action of the global gravity field:

$$\frac{d\mathbf{x}}{dt} = \frac{\mathbf{v}}{a} \quad (1)$$

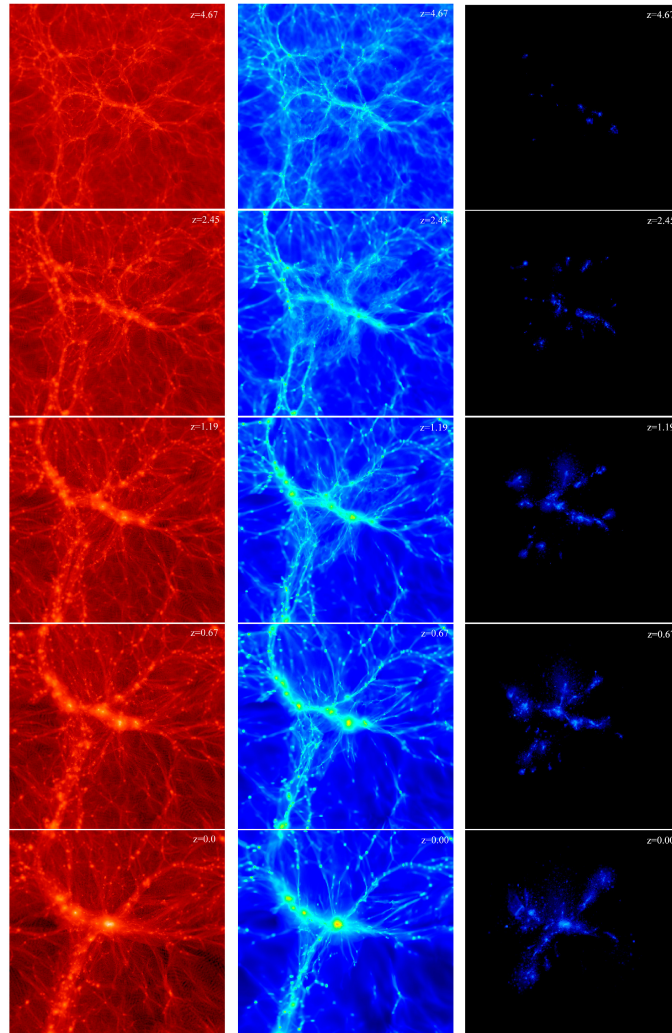


Figure 1: Formation and evolution of galaxy clusters in a hydrodynamical simulation performed with the Eulerian-AMR code MASCLLET [30]. The evolution of the dark matter, gas and stellar densities (left, central and right columns, respectively) from  $z \simeq 4$  until  $z = 0$  (panels from top to bottom) is shown. At  $z = 0$ , a big cluster with  $M_{vir} \sim 10^{15} M_{\odot}$  and  $R_{vir} \sim 3$  Mpc is formed. Each panel is a slice with a length of 64 comoving Mpc per edge and a depth of 5 comoving Mpc. Figure from [26].

$$\frac{d\mathbf{v}}{dt} = -\frac{\nabla\phi}{a} - H\mathbf{v}, \quad (2)$$

where  $\mathbf{x}$  and  $\mathbf{v} = a(t)\frac{d\mathbf{x}}{dt}$  represent, respectively, the comoving coordinates and the peculiar velocity of each particle,  $\phi(t, \mathbf{x})$  is the Newtonian gravitational potential, and  $a$ ,  $\rho_B$  and  $H$  are the scale factor, the background density and the Hubble constant. The solution of these equations can be found by integrating the Poisson's equation:

$$\nabla^2\phi = \frac{3}{2}H^2a^2\delta_T, \quad (3)$$

where the total density contrast,  $\delta_T$ , accounts for all the matter contributing to the density (both dark and baryonic matter). Once the global gravity field is known, the positions and velocities of each dark matter particle can be evolved.

The key of these N-body simulations relies on the computational technique employed to get the gravitational potential. The most direct and precise method consists in calculating the force among each pair of particles, being, however, computationally expensive when the number of particles is high. More refined schemes with a better compromise between resolution and computational cost have been also developed, such as the grid-based particle-mesh (PM) or the particle-particle/particle-mesh (P<sup>3</sup>M) methods, the gridless tree scheme, or a combination of several of these techniques.

- Gas hydrodynamics. If relativistic corrections are not needed, the evolution of cosmological inhomogeneities is usually described with the following equations [20]:

$$\frac{\partial\delta}{\partial t} + \frac{1}{a}\nabla \cdot (1 + \delta)\mathbf{v} = 0 \quad (4)$$

$$\frac{\partial\mathbf{v}}{\partial t} + \frac{1}{a}(\mathbf{v} \cdot \nabla)\mathbf{v} + H\mathbf{v} = -\frac{1}{\rho a}\nabla p - \frac{1}{a}\nabla\phi \quad (5)$$

$$\frac{\partial E}{\partial t} + \frac{1}{a}\nabla \cdot [(E + p)\mathbf{v}] = -3H(E + p) - H\rho\mathbf{v}^2 - \frac{\rho\mathbf{v}}{a}\nabla\phi \quad (6)$$

where  $\mathbf{x}$ ,  $\mathbf{v} = a(t)\frac{d\mathbf{x}}{dt}$ ,  $\rho$ ,  $\delta$ ,  $p$ , and  $E$  are, respectively, the coordinates, the peculiar velocity, the continuous density, the density contrast, the pressure, and the total energy density of the gaseous component. An equation of state, usually for an ideal gas, completes this system of equations. In this case, the evolution is driven by pressure gradients and gravitational forces. To obtain the source term  $\nabla\phi$ , Eqs. (4–6) have to be resolved together with Poisson's equation.

This set of hydrodynamical equations, which governs the evolution of the gaseous component, can be integrated using different numerical techniques. The use of a particular technique, with its inherent benefits and drawbacks, has a direct influence on the obtained results. These numerical techniques can be divided into three general families:

*Lagrangian or particle-based schemes.* In this numerical approach the fluid is represented by a set of gas particles. The Smooth Particles Hydrodynamics (SPH) [18, 14] is the most popular technique among this family of numerical schemes.

Given its relatively ease of implementation, its low computational cost, and its huge dynamical range, the SPH technique has been crucial in the last years, especially in simulations of cosmic structure formation. However, some of its undesirable features include (i) an imprecise treatment of shock waves, contact discontinuities and strong gradients, (ii) an inadequate description of low density domains, and (iii) the need of using artificial viscosity. Nowadays, however, a number of improvements to overcome some of these drawbacks have been successfully developed and implemented in some SPH codes [33, 35].

*Eulerian or grid-based shock-capturing methods.* Hydrodynamics is resolved on a computational grid of cells. Among the Eulerian schemes, those based on Riemann solvers have been very useful [32, 29, 8]. Some of the advantages of these numerical techniques are that, (i) they guarantee the numerical conservation of physical quantities, (ii) they generally resolve shocks, contact discontinuities and strong gradients accurately, (iii) they do not require the inclusion of numerical viscosity. An important weakness of this approach is that, in order to obtain a significant resolution, quite dense numerical grids are required, increasing significantly the computational cost. To overcome this problem allowing for a higher numerical resolution, the Adaptive Mesh Refinement (AMR) technique [4] is commonly used in order to refine the original computational grid only in regions of interest. Each one of the new refined grids (described with better resolution) represents a separated computational domain where the inherent properties of the Eulerian approach are still present. Another disadvantage associated to these numerical schemes is, for instance, the lack of Galilean-invariance. Some of the Eulerian-AMR hydrodynamical codes available nowadays for cosmological applications are, among others, those by [9] and [30].

*Moving Mesh or hybrid numerical schemes.* This is a kind of hybrid approach between Lagrangian and Eulerian schemes. It relies on a moving irregular mesh created by the Voronoi tessellation of a sample of points describing the simulation volume. The mesh is then employed to solve the hydrodynamical equations with an exact Riemann solver, in a similar way to Eulerian schemes. However, if the mesh-generating points move with the local flow velocity, this is a Lagrangian approach. This new technique is Galilean-invariant, it provides a huge dynamical range comparable to that of SPH codes, and it shows a high accuracy in the description of shocks and contact discontinuities. This approach has been recently implemented in the quasi-Lagrangian code AREPO [37].

These numerical techniques, with their associated strong and weak features, try to solve the same physical problems. However, given their properties, their accuracy in some physical applications can be quite different [2, 37]. Nevertheless, these approaches represent complementary and useful methods to resolve the hydrodynamical equations and to improve our knowledge of the physics affecting the gaseous component.

### 2.1.1 Non-gravitational physics

In general, hydrodynamical simulations accounting only for a non-radiative gas component are able of partially reproducing the self-similar scaling relations of galaxy clusters and groups; however, they still show some discrepancies with observations. In these adiabatic simulations, outer cluster regions ( $r \geq 0.1R_{vir}$ ) are nearly self-similar, reproducing quite well the observational data. However, cluster core regions and small groups and clusters show a larger scatter and significant departures from self-similarity. These deviations from a pure gravitational model suggest the effects of additional non-gravitational processes acting on the gas component. Indeed, cosmological simulations that try to reproduce in a consistent way the formation and evolution of cosmic structures (from the first galaxies to the most massive galaxy clusters) as well as the thermodynamical properties of the hot intra-cluster medium, need to include, besides gravitational physics, atomic and radiative processes.

Non-gravitational processes which are commonly included in state-of-the-art cosmological simulations are radiative cooling and heating for a primordial gas, star formation and its associated energy feedback, and metal production and chemical enrichment. Only recently it has been also possible to account for the effects of black hole growth with associated AGN feedback. Other studies have also included magnetic fields and additional non-thermal processes. In general, these processes are commonly included by means of relatively simple phenomenological parametrizations as extra terms in the energy equation (Eq. 6). An important complication in the modeling of these processes is that, in general, they require a subgrid-scale description, meaning that, while they are relevant on physical scales many orders of magnitude below the resolution limit of the simulations, their outcomes, such as radiation, thermal energy or heavy elements, are relevant on scales resolved by the simulations. Therefore, given the limited resolutions of current simulations, phenomenological models are needed to incorporate these mechanisms of energy feedback in a self-consistent way.

Gas radiative cooling should be present in any simulation aiming to reproduce the observed properties of galaxies and galaxy clusters. A desirable effect of cooling is that only high-entropy gas will be observed in X-rays. However, given that the fraction of condensed gas only depends weakly on cluster mass, cooling by itself can not break self-similarity as desired. In addition, it suffers from overcooling and, therefore, the fraction of cold gas converted into stars is much larger than observed. Moreover, the lack of central pressure support generated in cluster cores makes the gas from external regions to fall into the centre, increasing its temperature by adiabatic compression. To overcome the shortcomings associated to cooling, such as the lack of gas pressure in inner regions or the excessive star formation, a proper source of gas heating, or most likely a combination of several, has to be included. However, finding such a mechanism represents nowadays a major challenge in the field of numerical cosmology.

Given that an inherent product of the star formation process are SN-driven winds, SN feedback was early suggested as a mechanism to produce a genuine and self-regulated star formation [34]. SN explosions heat the surrounding medium and distribute metals from star-forming regions into the hotter ICM. In general, the inclusion of star formation and SN feedback in cosmological simulations partially counteracts radiative cooling, flattens the

cluster temperature profiles in the centre, and reduces the stellar mass fraction in clusters [7]. However, despite these beneficial effects of SN feedback, its low capability in compensating the cooling properly makes that the levels of core entropy still remain larger than observed, the brightest cluster galaxies (BCGs) also show larger stellar masses than reported by observations, and there exists an excess of metal production in cluster inner regions.

As suggested by cluster observations, AGN heating resulting from gas accretion onto a central supermassive black hole (SMBH) can significantly contribute to heat the ICM plasma, representing therefore the most likely source to explain the breaking of the ICM self-similar scaling relations as well as the cooling flow problem. Given its power and its self-regulated nature, AGN feedback can compensate radiative cooling in a natural way and reduce significantly the star formation in the BCGs. However, incorporating such a self-regulated process in simulations is quite challenging [7]. Only very recently it has been possible to include different models of AGN feedback in cosmological simulations (e.g. [36, 12, 31]). In these models, the rates of thermal AGN feedback injection are usually estimated using the Bondi gas accretion onto the central SMBHs [6]. Besides thermal feedback, kinetic AGN feedback in the form of relativistic jets can also contribute to shock and heat the ICM [3].

### 3 Present status of galaxy cluster cosmological simulations

In this Section, some of the results obtained from a set of hydrodynamical simulations of galaxy clusters including the aforementioned feedback mechanisms are shown. These simulations, performed with the parallel Tree-PM SPH code **GADGET-3** [35], consist in re-simulations of 29 Lagrangian regions chosen around massive DM halos formed in a lower resolution DM-only simulation. Three sets of these re-simulations have been performed including different prescriptions for the baryonic physics: (i) a set of non-radiative simulations (*NR*), (ii) a set of simulations including cooling, star formation, SN feedback and metal enrichment (*CSF*), and (iii) simulations including the same physical processes than the *CSF* runs but incorporating as well the effects of AGN thermal feedback (*AGN*). Each of this set of re-simulations contains a sample of about 160 groups and clusters with  $M_{vir} > 3 \times 10^{13} h^{-1} M_{\odot}$ . A detailed analysis of the ICM properties of this sample of clusters has been presented in [24] and [25]. We refer the reader to these references for further details on the physical results or on the technical specifications of these simulations.

As it is shown in the right panel of Fig. 2, AGN feedback seems to produce stellar mass fractions in better agreement with observations whereas the *CSF* simulations produce much larger values than observed. In addition, the left panel of Fig. 2 shows that AGN heating is also effective in reducing the amount of hot, X-ray emitting gas in small clusters and groups, producing therefore an  $L_X - T$  relation in better agreement with observations at all the mass range. Moreover, it has been shown that, as a consequence of the high efficiency of AGN feedback in dispersing heavy elements throughout the intra-cluster medium, it also helps in reproducing the observed profiles of ICM metallicity [12, 25].

Although the inclusion of AGN feedback seems to go in the right direction, a number of deviations between observed and simulated data still need to be addressed. As an example, as

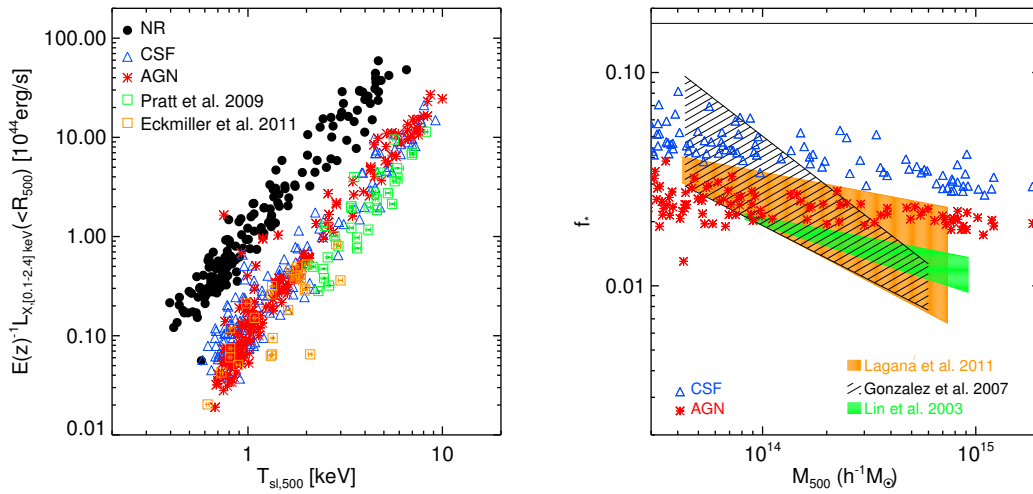


Figure 2: *Left panel:*  $L_X - T$  relation for the sample of groups and clusters identified in the simulations by [25]. Figure from [25]. *Right panel:* Stellar mass fraction as a function of cluster mass as obtained in the simulations by [24]. Figure from [24]. In both panels, different observational samples are included for comparison. See Section 3 for further details on the *NR*, *CSF* and *AGN* simulations.

it is shown in Fig. 3, simulated profiles of temperature and entropy for relaxed and unrelaxed systems are at variance with observations of cool core (CC) and non-cool core (NCC) clusters. These results suggest that the existing heating/cooling balance in cluster core regions is not yet properly reproduced by simulations including different prescriptions of baryonic physics. In addition, simulations still suffer from producing larger stellar masses of the BCGs than observed [31].

A number of recent studies (e.g. [13]) seem to indicate that, even with the inclusion of different models of kinetic or thermal AGN feedback, cosmological simulations are not able of breaking self-similarity to the observed level and simultaneously maintaining the cool-core structure of galaxy clusters and groups. This suggests that, in order to describe the main intra-cluster plasma properties from the core out to the outskirts of clusters, a proper AGN feedback model needs to be coupled with additional physical processes such as cosmic rays (CRs) in AGN-induced bubbles, heating induced by galaxy motions, or thermal conduction.

## 4 Final remarks

In the last years, cosmological hydrodynamical simulations together with supercomputing facilities have grown significantly, allowing us to understand in more detail the thermodynamical processes taking place within the hot intra-cluster medium and giving rise to the observational properties of galaxy clusters (see [17] and [26] for recent reviews).

In order to reproduce the observations, besides gravity, some non-gravitational pro-

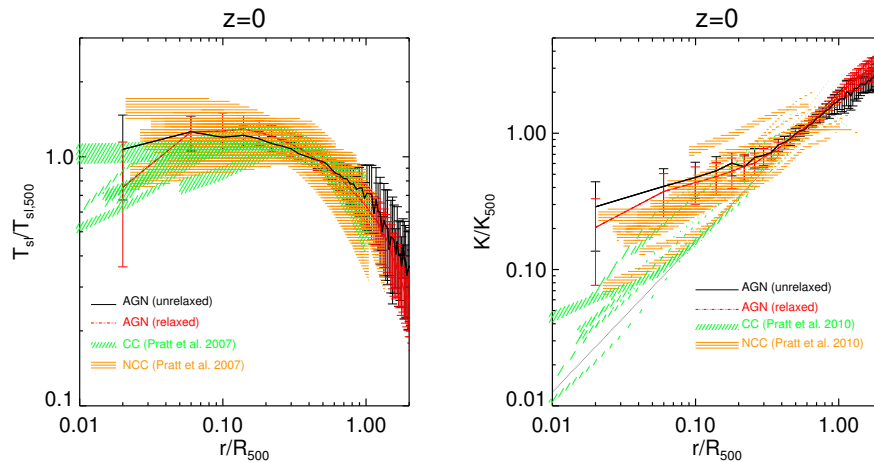


Figure 3: Left and right panels show, respectively, the mean temperature and entropy radial profiles obtained for the sample of relaxed/unrelaxed galaxy clusters within a set of simulations including AGN feedback (adapted from [25]). Radial profiles of CC and NCC clusters derived from X-ray observations [27, 28] are included for comparison. The self-similar prediction for the entropy is shown by the black dotted line ( $K \propto r^{1.1}$ ). Figure from [26].

cesses have been included in cosmological simulations. The non-gravitational processes usually taken into account are radiative cooling, star formation, SN feedback, and the effects of thermal and/or kinetic AGN feedback. In general, simulations including different prescriptions of these physical processes are able of reproducing most of the observational cluster properties, at least for high-mass clusters at intermediate cluster regions, where clusters behave in a nearly self-similar way. Nevertheless, cluster core regions ( $r \leq 0.2R_{500}$ ) and small groups and clusters present a number of complications that still need to be solved. In particular, due to an excess of gas cooling, simulations produce larger stellar and metal mass fractions than observed. Moreover, the cooling flow problem and the observed temperature and entropy radial profiles of CC and NCC clusters still need to be solved. On the other hand, however, a number of physical processes which usually are not included in simulations, such as cosmic rays or magnetic fields, can significantly affect cluster outskirts ( $r \geq R_{500}$ ), generating additional deviations from self-similarity.

This picture suggests that, although AGN feedback is considered to be an energy source capable of regulating radiative cooling in clusters, in addition to the standard physical processes already taken into account, additional mechanisms, such as thermal conduction or turbulence, must be also properly included. Therefore, a complex interplay between all these physical processes should be precisely understood and incorporated in simulations in order to explain the observational properties of galaxy clusters and groups.

In the next years, cosmological simulations are expected to be improved both in size and resolution and in a more precise treatment of the relevant non-gravitational physical processes explaining cluster observations. From an observational point of view, a larger number of clusters and groups will be provided by future instruments (such as *eROSITA*,

*Euclid* or *LSST*). These numerical and observational improvements are expected to help us to unravel the nature of the physical processes driving the formation of cosmic structures.

## Acknowledgments

This work has been supported by a grant funded by the “Consorzio per la Fisica di Trieste”. SP also acknowledges support by the PRIN-INAF09 project “Towards an Italian Network for Computational Cosmology”, by the PRIN-MIUR09 “Tracing the growth of structures in the Universe”, and by the PD51 INFN grant. This work has been also partially supported by *Spanish Ministerio de Ciencia e Innovación* (MICINN) (grants AYA2010-21322-C03-02 and CONSOLIDER2007-00050).

## References

- [1] Aarseth S. J. 1963, MNRAS 126
- [2] Agertz O. et al. 2007, MNRAS, 380, 963
- [3] Barai P., Viel M., Murante G., Gaspari M., & Borgani S. 2013, MNRAS, 437, 1456
- [4] Berger M. J. & Olinger J. 1984, J. Comp. Phys., 53, 484
- [5] Blumenthal G. R., Faber S. M., Primack J. R., & Rees M. J. 1984, Nature, 311, 517
- [6] Bondi H. 1952, MNRAS, 112, 195
- [7] Borgani S. & Kravtsov A. 2011, Advanced Science Letters, 4, 204.
- [8] Bryan G. L., Norman M. L., Stone J. M., Cen R. & Ostriker J. P. 1995, Computer Physics Communication, 89, 149
- [9] Bryan G. L. & Norman M. L. 1997, ASP Conf. Ser. 123, 363
- [10] Dolag K., Borgani S., Schindler S., Diaferio A., & Bykov A. M. 2008, SSR, 134, 229.
- [11] Evrard A. E. 1988, MNRAS 235, 911
- [12] Fabjan D., Borgani, S., Tornatore L., Saro A., Murante G., & Dolag K. 2010, MNRAS, 401, 1670
- [13] Gaspari M., Brighenti F., Temi P. & Ettori S. 2014, ApJL, 783, L10
- [14] Gingold R. A. & Monaghan J.J. 1977, MNRAS, 181, 375
- [15] Hernquist L. & Katz N. 1989, ApJS, 70, 419
- [16] Kaiser N. 1986, MNRAS, 222, 323
- [17] Kravtsov A. V. & Borgani S. 2012, ARAA, 50, 353
- [18] Lucy L. B. 1977, AJ, 82, 1013
- [19] Peebles, P. J. E. 1970, AJ, 75, 13
- [20] Peebles, P. J. E. 1980, Princeton University Press
- [21] Planck Collaboration, Paper XVI. 2013, arXiv-1303.5076
- [22] Planelles S., & Quilis V. 2009, MNRAS 399, 410
- [23] Planelles S., & Quilis V. 2013, MNRAS 428, 1643

- [24] Planelles S., Borgani S., Dolag K., Ettori S., Fabjan D., Murante G., & Tornatore L. 2013, MNRAS, 431, 1487
- [25] Planelles S., Borgani S., Fabjan D., Killeidar M., Murante G., Granato G.L., Ragone-Figueroa C., & Dolag K. 2014, MNRAS, 438, 195
- [26] Planelles S., Schleicher D.R.G., & Bykov A.M. 2014, Space Sci Rev, DOI 10.1007/s11214-014-0045-7
- [27] Pratt G. W., Böhringer H., Croston J. H., Arnaud M., Borgani S., Finoguenov A., Temple R.F. 2007, A&A, 461, 71
- [28] Pratt G. W., Arnaud M., Piffaretti R., Böhringer H., Ponman T.J., Croston J. H., Voit G. M., Borgani S., Bower R. G.. 2010, A&A, 511, A85
- [29] Quilis V., Ibáñez J.M. & Sáez D. 1994, A&A, 286, 1
- [30] Quilis V. 2004, MNRAS 352, 1426
- [31] Ragone-Figueroa C., Granato G. L., Murante G., Borgani S., & Cui W. 2013, MNRAS, 436, 1750.
- [32] Ryu D., Ostriker J. P., Kang H. & Cen R. 1993, ApJ, 414, 1
- [33] Springel V., Yoshida N., White S. D. M. 2001, New Astronomy, 6, 79
- [34] Springel V. & Hernquist L. 2003, MNRAS, 339, 289
- [35] Springel V. 2005, MNRAS, 364, 1105
- [36] Springel V., Di Matteo T., & Hernquist L. 2005, MNRAS, 361, 776
- [37] Springel, V. 2010, MNRAS, 401, 791